DOI: 10.1002/eji.201948164 Eur. J. Immunol. 2019. 49: 2012–20

European Journal of Immunology

Innate immunity

Short Communication

Mesothelial cell CSF1 sustains peritoneal macrophage proliferation

Stoyan Ivanov[*1], *Alexandre Gallerand*[*1], *Marilyn Gros*[*2], *Marion I. Stunault*[1], *Johanna Merlin*[1], *Nathalie Vaillant*[1], *Laurent Yvan-Charvet*[1] *and Rodolphe R. Guinamard*[1]

[1] Centre méditerranéen de médecine moléculaire, Université Côte d'Azur - INSERM, U1065, Team 13, Nice, France
[2] Muscle & ALS Department, Centre Hospitalier Universitaire de Nice, Université Côte d'Azur, Peripheral Nervous System, Pasteur 2 Hospital, Nice, France

Macrophages play a central role during infection, inflammation and tissue homeostasis maintenance. Macrophages have been identified in all organs and their core transcriptomic signature and functions differ from one tissue to another. Interestingly, macrophages have also been identified in the peritoneal cavity and these cells have been extensively used as a model for phagocytosis, efferocytosis and polarization. Peritoneal macrophages are involved in B-cell IgA production, control of inflammation and wound healing following thermal-induced liver surface injury. These cells presumably require and interact with the omentum, where milky spot stromal cells have been proposed to secrete CSF1 (colony stimulating factor 1). Peritoneal macrophages depend on CSF1 for their generation and survival, but the identity of CSF1 producing cells inside the large peritoneal cavity remains unknown. Here we investigated peritoneal macrophage localization and their interaction with mesothelial cells, the major cell type predicted to secrete CSF1. Our data revealed that mesothelial cells produce membrane bound and secreted CSF1 that both sustain peritoneal macrophage growth.

Keywords: CSF1 · mesothelial cell · peritoneal macrophage

Additional supporting information may be found online in the Supporting Information section at the end of the article.

Introduction

The peritoneal cavity hosts several myeloid cell populations including large peritoneal macrophages (LPMs) and small peritoneal macrophages (SPMs). These two populations express the markers CD64 (the high affinity IgG receptor) and MerTK that are conserved in all tissue resident macrophages [1]. Nevertheless, LPMs are characterized by a high CD102 (ICAM-2) and F4/80 expression that distinguish them from SPMs [2]. Large peritoneal macrophages are arguably the most studied population of tissue resident macrophages. The transcription factor Gata6 controls their development in a vitamin A-dependent manner [3–5]. However, little is known about LPMs localization inside the peritoneal cavity and whether a tissue specific tropism exists. The peritoneal cavity has an estimated surface area equivalent to skin and represents the largest serous membrane in the body [6]. A single layer

Correspondence: Dr.Stoyan Ivanov and Rodolphe R. Guinamard
e-mail: stoyan.ivanov@unice.fr; rodolphe.guinamard@unice.fr

*These authors equally contributed to this work.

of mesothelial cells (MCs) covers the stratum of connective tissue inside the peritoneal cavity and constantly secretes fluid acting as lubricate and facilitating inter-organ frictions [6]. LPMs depend on the growth factor CSF1 for their survival and express high levels of its receptor CSF1R (CD115) on their cell surface [2, 7]. CSF1 is crucial for both monocyte survival and tissue resident macrophage maintenance [8, 9]. Peritoneal macrophages are completely absent in osteopetrotic op/op mice, presenting a spontaneous mutation in the CSF1 gene and lacking functional protein [10–12]. Nevertheless, the cellular source of CSF1 inside the peritoneal cavity remains currently unknown. Our data revealed that mesothelial cells produce CSF1 and induce peritoneal macrophage proliferation likely contributing to their homeostatic maintenance.

Results and discussion

Recently generated publicly available single cell transcriptional analysis data [13] (Tabula Muris Consortium) revealed that adipose tissue mesenchymal precursor cells, mammary gland epithelial cells, bladder cells, non-myeloid brain cells and blood endothelial cells selectively express CSF1 mRNA in comparison to other stromal and immune cells (Fig. 1A and B). Since adipose tissue blood endothelial cells are not directly connected with the peritoneal cavity, this suggests that adipose tissue mesenchymal cells, including cells with mesothelial markers such as mesothelin and WT1, are likely the major cell type producing CSF1 inside the peritoneal cavity. Another candidate is neutrophil-derived CSF1 as those cells were shown to stimulate macrophage proliferation [14]. This is rather unlikely to occur inside the peritoneal cavity since neutrophils are barely present at steady state in this location (65% LPMs against 0.4% neutrophils among $CD45^+$ cells in our colony, data not shown). We analyzed whether LPMs are present at the outer surface of an intraperitoneal organ, the epididymal adipose tissue (eAT). To document cell topology, we injected i.p. labelled antibodies directed against hematopoietic cells (anti-CD45) and mesothelial cells (anti-podoplanin (Pdpn)) and analyzed mice 5 min post-antibody administration. eAT was excised and submitted to a brief surface trypsin digestion, a process known to liberate mesothelial cells, and then fully digested with collagenase A (Fig. 1C). Trypsin digestion resulted in a large fraction of $CD45^-CD31^-CD90^+$ cells that was accessible to the i.p. injected anti-Pdpn, and its surface location and phenotype is reminiscent of mesothelial cells. Trypsin failed to digest endothelial cells as revealed by the small $CD45^-CD31^+CD90^-$ fraction (Fig. 1D). By contrast, collagenase A liberated a large endothelial cell fraction that were not stained by the i.p. injected anti-Pdpn. Among $CD45^+$ cells, surface trypsin digestion liberated preferentially a population of $CD45^+CD11b^{bright}F4/80^{bright}$ cells that stained positive for ICAM-2 and was accessible to the i.p. injected anti-CD45 and very few to none $CD45^+CD11b^{hi}F4/80^{int}$ cells (Fig. 1D). The latter population was recovered preferentially after a full enzymatic digestion and stained negative for ICAM-2 and the injected anti-CD45. Altogether, this suggests that the ICAM-2^+ population resides inside the peritoneal cavity and represents a fraction of the LPM pool (Fig. 1D). We sought to determine whether those LPMs are tightly associated to adipose tissue mesothelial cells. We collected both eAT pads, washed one and compared it to the non-washed control pad. Flow cytometry analysis revealed that the peritoneal macrophage population ($CD64^+F4/80^+$ICAM-2^+) at the outer surface of eAT was lost following PBS wash, suggesting that the interaction, if any, between LPMs and mesothelial cells was rather loose (Fig. 1E and F). By contrast, omentum residing LPMs were not removed following the washing procedure (Fig. 1E and F). The population of adipose tissue macrophages (non-LPMs in eAT) was not affected by the lavage confirming that these cells reside inside the organ (Fig. 1F).

To better apprehend the mesothelial cells-LPMs dialogue, we developed a co-culture system between these two cell types. Mesothelial cell identity was confirmed using microscopy that revealed the typical pavementous morphology of these cells and Pdpn staining (Fig. 2A and not shown). Total cells were extracted from the peritoneal cavity of $Lyz2^{cre} \times TdTomato^{fl/fl}$ mice and macrophages were followed by counting $Tomato^+$ cells using Incucyte live imaging system. Over a period of 8 days, LPMs exponentially increased in the presence of mesothelial cells while they were lost when grown among their co-inhabitants of the peritoneal cavity (Fig. 2A and B). We confirmed cell identities in the co-culture using CD90/Pdpn staining for mesothelial cells and Lyz2 reporter together with CD11b, F4/80, CD64 and MerTK for LPMs (Fig. 2C and not shown). These data confirmed LPM expansion (100% $Tomato^+$ are $F4/80^+CD64^+CD11b^+$ $MerTK^+$ cells, Fig. 2C and 2H) in the presence of mesothelial cells that likely produced a growth factor supporting their proliferation. Such dynamic interaction between two cell types was recently reported between fibroblasts and macrophages [15]. CSF1 protein was secreted by mesothelial cells as revealed by ELISA test (Fig. 2D). Both adipose tissue and liver-derived mesothelial cells produced CSF1 and its concentration strongly decreased when LPMs were added to the culture, suggesting that the latter ones are consuming large amounts of CSF1 (Fig. 2D). Of interest, the addition of CSF1R-neutralizing antibody completely prevented LPMs proliferation, demonstrating the dominance of the CSF1-CSF1R axis in our system (Fig. 2E). This was paralleled by increased CSF1 concentration in the co-culture supernatants when CSF1R-neutralizing antibody was added (Fig. 2F). Bone marrow contains a large monocyte fraction expressing CSF1R and known to respond to CSF1 stimulation [9]. To test the prediction that mesothelial cell would promote their expansion, we added bone marrow cells (BMs) on top of adipose tissue mesothelial cells and we observed an impressive expansion of $Tomato^+$ BM cell (Fig. 2G). This dataset suggests that mesothelial cells can, by mean of CSF1 production, stimulate the proliferation of any CSF1R-expressing cells with no particular specificity for LPMs. Further analysis of mesothelial cell/peritoneal cell co-cultures revealed that all $TdTomato^+$ cells stained positive for F4/80 and CD11b but were $CX3CR1^{low}$, suggesting that after 8 days of co-culture LPMs kept their typical phenotypic markers (Fig. 2H). Interestingly, when BM cells were co-cultured with mesothelial cells, all $TdTomato^+$ cells were $F4/80^+$ and $CD11b^+$

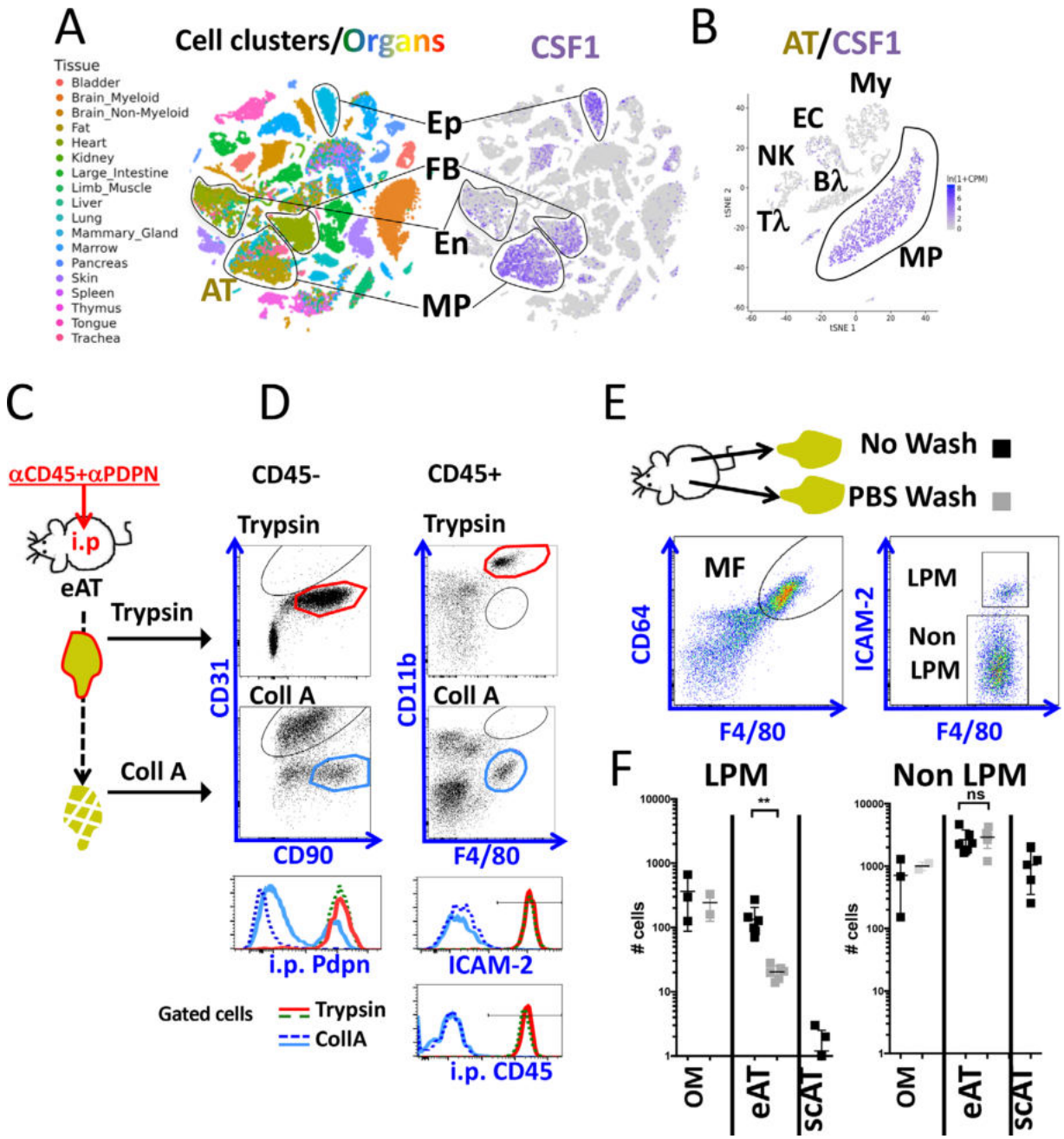

Figure 1. Transcriptional analysis of CSF1 mRNA across tissues and potential role for LPMs maintenance. (A) Clusters corresponding to major cell types expressing CSF1 are boxed as Ep (Epithelial cells), FB (Fibroblast), EC (Endothelial cell) and MP (Mesenchymal Precursor cells). Color code refers to organ of origin according to the presented list (left panel). (B) Focus on adipose tissue, with major cell type clusters highlighted. My: myeloid cell; EC; NK: Natural Killer cell; B: B cell; T: T cell and MP. (C) Experimental design includes 5-min intra-peritoneal injection of 1 μg of PE-(Phycoerythrin) labelled anti-CD45 antibody together with 1 μg of APC-Cy7 labelled anti-Pdpn, surface tryptic digestion of full tissue (surface digestion) followed by mincing and collagenase A digestion (2nd digestion). (D) Dot plot representing CD90 versus CD31 staining of $CD45^-$ cells and staining by the i.p. injected anti-Pdpn of the $CD45^-CD90^+CD31^-$ gated populations and dot plot of F4/80 and CD11b staining of $CD45^+$ cells with further staining for ICAM-2 and injected i.p. anti-CD45 of the gated populations. (red boxed $F4/80^{bright}CD11b^{bright}$ cells from tryptic digestion and blue boxed $F4/80^{int}CD11b^{hi}$ cells from collagenase A digestion), the experiment presented compares two injected mice and is one representative experiment of three (2–6 mice per experiment with similar results). (E) Experimental design and gating strategies. Epididymal adipose tissue (eAT), omentum (OM) and subcutaneous adipose tissue (scAT) were either digested in collagenase A directly or after 4 PBS washes. Dot plot representing gating strategy that includes $CD64^+F4/80^+$ macrophages and further ICAM-2 staining, allowing the separation of LPMs ($ICAM\text{-}2^+$) and (non-LPM) ($ICAM\text{-}2^-$). (F) LPM and non-LPM quantification per organ is presented, each symbol representing one organ (black symbols = not washed, grey symbols = washed) (F was performed using 5 mice and repeated once with 6 mice and similar results; ns = non-significant, ** = $p < 0.005$ with two tailed non-parametric t-test followed by Mann–Whitney test).

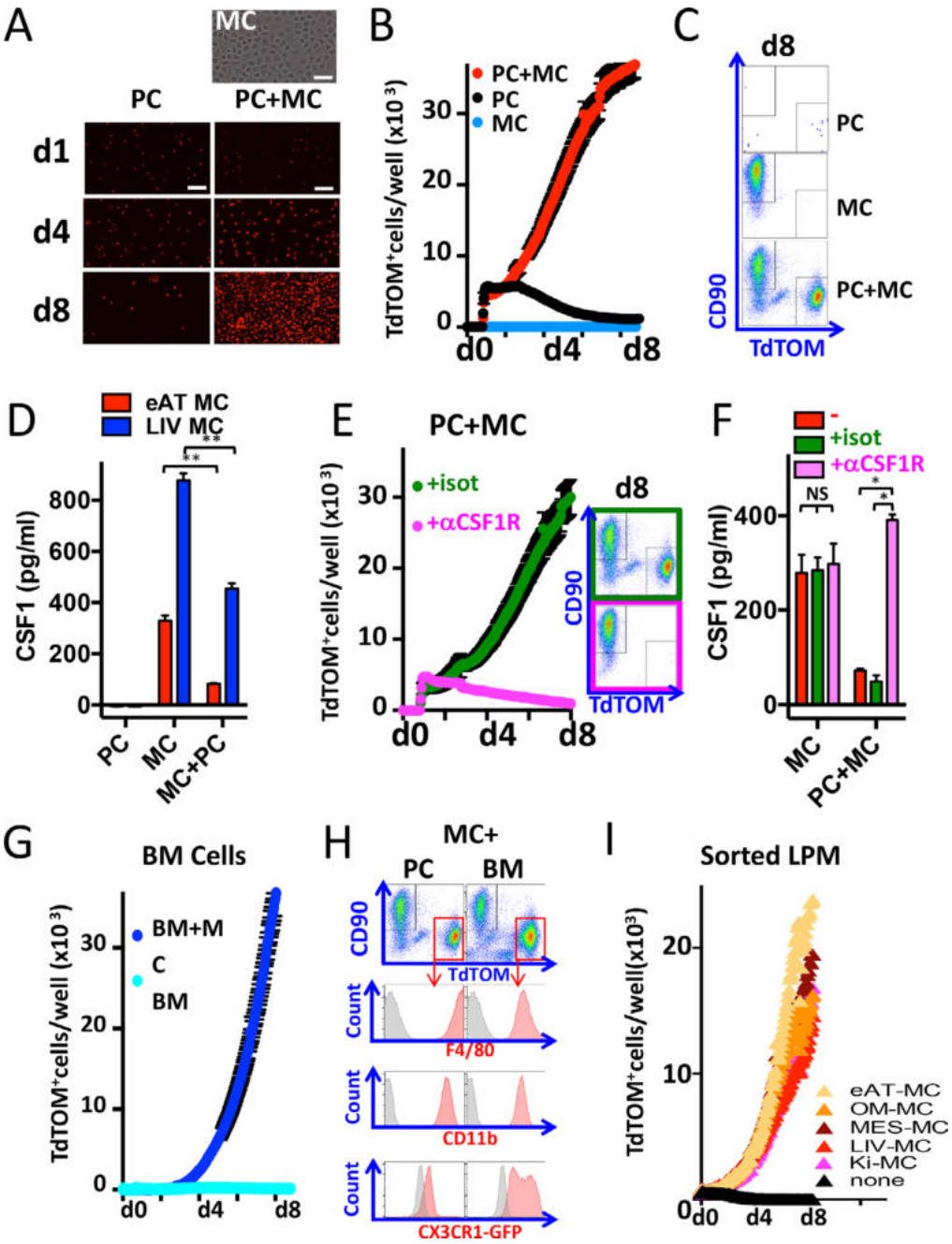

Figure 2. Mesothelial cells promote CSF1 dependent myeloid cell proliferation. 200 000 mesothelial cells (MC) were plated at day 0 and overlayed with 100 000 peritoneal cells (PCs) isolated from $Lyz2^{cre} \times TdTomato^{fl/fl}$ /$CX3CR1^{GFP}$ mice. Macrophage growth with or without MC was documented in real time by counting $Tomato^{+}$ fluorescent cells; (A) Representative pictures of red fluorescence ($TdTomato^{+}$ cells) at indicated times; top panel, exemplifies MC morphology. (Scale bar = 100 μm) (B) Real time quantification of macrophage growth ($TdTomato^{+}$ cells per well of a 24-well plate); (C) Dot plot showing CD90 versus TdTomato staining of live cells at the end of the co-culture (Day 8). (D) CSF1 quantification by ELISA test during 96 h of PCs, MCs and PCs+MCs co-cultures. (E) As described in 2A/B/C with the addition of blocking anti-CSF1R monoclonal antibody (10 μg/mL) or isotype control at day 1 of culture. (F) PCs + MCs co-cultures were first established for 4 days before medium was exchanged and replaced by medium with or without anti-CSF1R or isotype control, and supernatants were taken 3 days later and analyzed for CSF1 by ELISA. (G) As described in 2B, except that total bone marrow was used. (H) Staining of day 8 MCs + PCs or BMs co-cultures, CD90 vs TdTomato dot plot of live cells is presented as well as F4/80, CD11b and $CX3CR1^{GFP}$ staining of the $CD90^{-}$ $TdTomato^{+}$ population. (I) MCs were generated by organ surface trypsin digestion from epididymal adipose tissue (eAT), omentum (OM), mesenteric adipose tissue (MES), liver (LIV) and kidney (Ki). Cell-sorted LPMs obtained from $Lyz2^{cre} \times TdTomato^{fl/fl}$ mice (1×10^4 cells) were then added. One representative experiment is presented out of four for LPM growth and out of two for ELISA tests and blocking anti-CSF1R assay. All experiments were done at least three times except for 2I that was done twice. Two tailed non-parametric t-test followed by Mann–Whitney test was performed with GraphPad Prism 6 software to test the samples statistical significance ($^{*}p < 0.05$; $^{**}p < 0.01$).

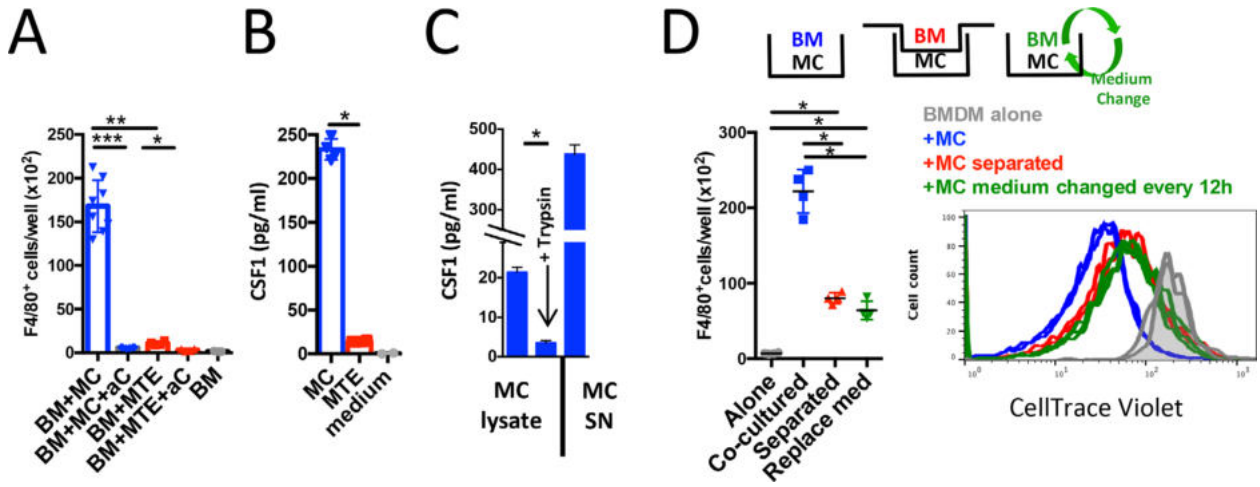

Figure 3. Cell-contact and secretion control CSF1 dependent myeloid cell proliferation. (A) 10 000 mesothelial cells (MC) or MTE4.14 (MTE) thymic stromal cells were plated at day 0 and overlayed 24 h later with 5000 BMDMs. At day 7, cells were stained for F4/80 and CD45 and the number of $CD45^+F4/80^+$ cells was counted. (B) CSF1 was measured in the supernatant of eAT MC and MTE cells cultured for 3 days. (C) eAT MC co-culture supernatant (MC SN) was collected, cells washed 3x with PBS and either lysed directly in RIPA buffer (MC lysate) or following a 5-min surface trypsin digestion. Data shown are from quadruplicates of one representative of two experiments. (D) 400 000 eAT MCs were plated at day 0 in 6-well plates. 48 h later, 100 000 violet proliferation dye stained BM cells were either co-cultured in the same well or placed on 0.4 μM transwell inserts (Greiner). In half of the co-culture wells culture supernatant was removed completely and replaced with fresh medium every 12 h. After 6 days, the number of live $F4/80^+$ was counted and violet staining of $F4/80^+$ cells in different conditions was plotted (values are of triplicates, with 2 experiments performed). Two tailed non-parametric *t*-test followed by Mann–Whitney test was performed with GraphPad Prism 6 software to test the samples statistical significance (*$p < 0.05$; **$p < 0.01$; ***$p <$ 0,001).

but a fraction was $CX3CR1^{gfp+}$ as well, suggesting a diversity in these cells (Fig. 2H). Given that both liver and adipose tissue mesothelial cells were able to sustain CSF1 dependent growth, we hypothesized that this might represent a conserved function of all peritoneal organ mesothelial cells. We found that all peritoneal mesothelial cells that we tested were capable of sustaining LPMs growth. This ubiquitous ability to grow myeloid cells was not shared by a thymic stromal cell line or by culturing large amount of bone marrow, blood or peritoneal cells that contains numerous diverse cell types (Fig. 3A and not shown). Thymic stromal cells produced few CSF1 in comparison to mesothelial cells (Fig. 3B). CSF1 is produced in 3 different biologically active isoforms including a membrane-spanning glycoprotein, a secreted proteoglycan and a secreted glycoprotein [16]. We tested for the presence of a membrane bound isoform by dosing CSF1 in mesothelial cell lysates. We detected a trypsin sensitive cell-associated CSF1 in lysates (~20 pg/mL), even thought the amount was lower in comparison to the secreted form found in cell-culture supernatants (~450 pg/mL) (Fig. 3C). Finally, we tested whether LPM proliferation requires cell–contact interaction or, alternatively, is mediated by secreted CSF1. We performed Transwell assay in which mesothelial cells were seeded in the bottom and BM cells added to the upper well (Fig. 3D). Surprisingly, and despite the large amount of CSF1 detected in the culture supernatant, BM cell proliferation was largely blunted when physically separated from mesothelial cells (Fig. 3D). Also, to test for the importance of the soluble form, culture supernatant was replaced every 12 h with fresh medium, a similar strong decrease in myeloid cell proliferation was measured. Our data suggest that both membrane and secreted factors including CSF1 are present and secreted by mesothelial cells that can induce macrophage proliferation (Fig. 3C and D). Mice expressing only one CSF1 isoform have been previously generated [17, 18] but how this affects LPMs proliferation remains currently unknown.

Taken together, we defined peritoneal mesothelial cells as a major source of CSF1 and critical contributor to peritoneal macrophage homeostasis. Currently, there is an urgent need to generate mouse genetic model to validate our finding that mesothelial cells-derived CSF1 contributes to peritoneal macrophage survival. Indeed, we are not aware of mesothelial cell specific Cre mouse model that can be crossed to CSF1 floxed mice [19] and validate our findings in vivo. Mesothelin-driven Cre expression in mice is not exclusively restricted to mesothelial cells but also affects, among others, hepatic portal fibroblasts [20, 21]. Nevertheless, we believe that our study reveals a new role for mesothelial cells. By CSF1 production, these cells potentially contribute to peritoneal macrophage pool maintenance.

Concluding remarks

In the present study we described an unprecedently attributed function of peritoneal mesothelial cells. By secreting CSF1 they sustain peritoneal macrophage proliferation. This interaction is completely CSF1R dependent as illustrated by the addition of neutralizing antibody. Both cell contact between mesothelial cells and LPMs and CSF1 secretion are required for optimal macrophage proliferation. This might explain differential myeloid cell turn-over upon steady versus injury conditions that promote adhesion [22].

Materials and methods

$Lyz2^{Cre}$ mice (B6.129P2-Lyz2tm1(cre)Ifo/J, The Jackson Laboratory) have been crossed to TdTomato reporter mice (B6.Cg-Gt(ROSA)26Sortm9(CAG-tdTomato)Hze/J, The Jackson Laboratory) and $CX3CR1^{gfp}$ mice (B6.129P-$Cx3cr1^{tm1Litt}$/J, The Jackson Laboratory). Animal protocols were approved by the Institutional Animal Care and Use Committee of the French Ministry of Higher Education and Research and the Mediterranean Center of Molecular Medicine (Inserm U1065) and were undertaken in accordance with the European Guidelines for Care and Use of Experimental Animals. Animals had free access to food and water and were housed in a controlled environment with a 12-h light– dark cycle and constant room temperature (22°C).

Flow cytometry

Tissues were collected, and surface digested or not with Trypsin before shredding and then incubating for 30 min at 37°C with RPMI medium containing 2 mg/mL collagenase A (Roche Diagnostics). Following red blood cells were lysed (BD Pharmlyse), cells were centrifuged (400 g, 5 min at 4°C) and stained for 25 min on ice. Stained cells were acquired on a BDFACSCanto flow cytometer. Analysis was performed using FlowJo software (Tree Star). The authors adhered and followed the guidelines described in 'Guidelines for the use of flow cytometry and cell sorting in immunological studies'.

Antibodies and reagents

The following list of reagents and antibodies was used: rCSF1 (Miltenyi); ICAM-2-APC conjugated (clone 3C4(mIC2/4), BioLegend); CD11b-APC-Cy7 conjugated (clone M1/70, BioLegend); F4/80-Pe-Cy7 conjugated (clone BM8, BioLegend); Podoplanin-FITC or APC-Cy7 -conjugated (clone 8.1.1, BioLegend); CD90.2-BrilliantViolet510 conjugated (clone 53-2.1, BioLegend); CD31-PerCP-Cy5.5 conjugated (clone 390, Biolegend); CD45-PE conjugated (clone 30-F11, BioLegend); CD64-BrilliantViolet421 conjugated (clone X54-5/7.1, BioLegend); CSF1R-neutralizing antibody (BioXcell); rat IgG2b isotype control (BioXcell); Mouse M-CSF Quantikine ELISA Kit (R&D Systems). LIVE/DEAD® Fixable Aqua Dead Cell Stain Kit and CellTrace Violet Cell Proliferation Kit were purchased from ThermoScientific and used according to the manufacturer's instruction.

Peritoneal macrophage generation

Peritoneal lavage was performed with 5 mL of FACS Buffer (RPMI medium, 0.3 mM EDTA and 0.06% BSA). Cells were centrifuged for 5 min at 1500 rpm at 4°C, counted and used in various experiments.

Incucyte

Adipose tissue and liver were collected, washed in PBS 1x and the surface was digested with Trypsin-EDTA 0,05% (Gibco) for 10 min at 37°C. Cells were cultured as previously described [23]. Cells were counted and plated at $2*10^5$ cells per well in 24-well tissue culture plates for 24 h. Macrophages and BM cells ($1*10^5$ cells) were then added. Photomicrographs were taken every hour using an Incucyte live cell imager (Essen Biosciences) for 8 days and tomato positive cells number were counted using Incucyte software (Essen Biosciences).

Statistical analyses

Statistical analyses were generated with GraphPad Prism software using statistical tests indicated for each experiment.

Acknowledgements: We would like to thank Julie Gall, Marion Ayrault, Emma Guilbaud and Gaël Bories for their technical assistance and helpful discussions and Philippe Gual for sharing $CD44^{-/-}$ mice. SI is supported by Institut National de la Sante et de la Recherche Medicale (INSERM) and Agence Nationale de la Recherche (ANR-17-CE14-0017-01). LYC is supported by Institut National de la Sante et de la Recherche Medicale (INSERM), Fondation de France (00066474) and the European Research Council (ERC) consolidator program (ERC2016COG724838). RRG is supported by Centre National de la Recherche Scientifique (CNRS).

Authorship contributions: SI and RG designed and performed experiments, analyzed the data and wrote the manuscript. AG, MJG, MIS, JM and NV performed experiments, analyzed data and edited the manuscript. LYC supervised the project and edited the manuscript.

Conflicts of interest: The authors have no disclosures or conflicts of interest to declare.

References

1 **Gautier, E. L., Shay, T., Miller, J., Greter, M., Jakubzick, C., Ivanov, S., Helft, J. et al.**, Gene-expression profiles and transcriptional regulatory pathways that underlie the identity and diversity of mouse tissue macrophages. *Nat. Immunol.* 2012. **13**: 1118–1128.

2 **Kim, K. W., Williams, J. W., Wang, Y. T., Ivanov, S., Gilfillan, S., Colonna, M., Virgin, H. W. et al.**, MHC II+ resident peritoneal and pleural macrophages rely on IRF4 for development from circulating monocytes. *J. Exp. Med.* 2016. **213**: 1951–1959.

3 **Rosas, M., Davies, L. C., Giles, P. J., Liao, C. T., Kharfan, B., Stone, T. C., O'Donnell, V. B. et al.**, The transcription factor Gata6 links tissue macrophage phenotype and proliferative renewal. *Science* 2014. **344**: 645–648.

4 **Gautier, E. L., Ivanov, S., Williams, J. W., Huang, S. C., Marcelin, G., Fairfax, K., Wang, P. L. et al.**, Gata6 regulates aspartoacylase expression in resident peritoneal macrophages and controls their survival. *J. Exp. Med.* 2014. **211**: 1525–1531.

5 **Okabe, Y. and Medzhitov, R.**, Tissue-specific signals control reversible program of localization and functional polarization of macrophages. *Cell* 2014. **157**: 832–844.

6 **van Baal, J. O., Van de Vijver, K. K., Nieuwland, R., van Noorden, C. J., van Driel, W. J., Sturk, A., Kenter, G. G. et al.**, The histophysiology and pathophysiology of the peritoneum. *Tissue. Cell* 2017. **49**: 95–105.

7 **Gautier, E. L., Ivanov, S., Lesnik, P. and Randolph, G. J.**, Local apoptosis mediates clearance of macrophages from resolving inflammation in mice. *Blood* 2013. **122**: 2714–2722.

8 **Louis, C., Cook, A. D., Lacey, D., Fleetwood, A. J., Vlahos, R., Anderson, G. P. and Hamilton, J. A.**, Specific contributions of CSF-1 and GM-CSF to the dynamics of the mononuclear phagocyte system. *J. Immunol.* 2015. **195**: 134–144.

9 **Yona, S., Kim, K. W., Wolf, Y., Mildner, A., Varol, D., Breker, M., Strauss-Ayali, D. et al.**, Fate mapping reveals origins and dynamics of monocytes and tissue macrophages under homeostasis. *Immunity* 2013. **38**: 79–91.

10 **Yoshida, H., Hayashi, S., Kunisada, T., Ogawa, M., Nishikawa, S., Okamura, H., Sudo, T. et al.**, The murine mutation osteopetrosis is in the coding region of the macrophage colony stimulating factor gene. *Nature* 1990. **345**: 442–444.

11 **Naito, M., Kodama, T., Matsumoto, A., Doi, T. and Takahashi, K.**, Tissue distribution, intracellular localization, and in vitro expression of bovine macrophage scavenger receptors. *Am. J. Pathol.* 1991. **139**: 1411–1423.

12 **Wiktor-Jedrzejczak, W. W., Ahmed, A., Szczylik, C. and Skelly, R. R.**, Hematological characterization of congenital osteopetrosis in op/op mouse. Possible mechanism for abnormal macrophage differentiation. *J. Exp. Med.* 1982. **156**: 1516–1527.

13 **The Tabula Muris Consortium**, Single-cell transcriptomics of 20 mouse organs creates a Tabula Muris. *Nature* 2018. **562**: 367–372.

14 **Braza, M. S., Conde, P., Garcia, M., Cortegano, I., Brahmachary, M., Pothula, V., Fay, F. et al.**, Neutrophil derived CSF1 induces macrophage polarization and promotes transplantation tolerance. *Am. J. Transplant.* 2018. **18**: 1247–1255.

15 **Zhou, X., Franklin, R. A., Adler, M., Jacox, J. B., Bailis, W., Shyer, J. A., Flavell, R. A. et al.**, Circuit design features of a stable two-cell system. *Cell* 2018. **172**: 744–757 e717.

16 **Pixley, F. J. and Stanley, E. R.**, CSF-1 regulation of the wandering macrophage: complexity in action. *Trends. Cell. Biol.* 2004. **14**: 628–638.

17 **Dai, X. M., Zong, X. H., Sylvestre, V. and Stanley, E. R.**, Incomplete restoration of colony-stimulating factor 1 (CSF-1) function in CSF-1-deficient Csf1op/Csf1op mice by transgenic expression of cell surface CSF-1. *Blood* 2004. **103**: 1114–1123.

18 **Ryan, G. R., Dai, X. M., Dominguez, M. G., Tong, W., Chuan, F., Chisholm, O., Russell, R. G. et al.**, Rescue of the colony-stimulating factor 1 (CSF-1)-nullizygous mouse (Csf1(op)/Csf1(op)) phenotype with a CSF-1 transgene and identification of sites of local CSF-1 synthesis. *Blood* 2001. **98**: 74–84.

19 **Harris, S. E., MacDougall, M., Horn, D., Woodruff, K., Zimmer, S. N., Rebel, V. I., Fajardo, R. et al.**, Meox2Cre-mediated disruption of CSF-1 leads to osteopetrosis and osteocyte defects. *Bone* 2012. **50**: 42–53.

20 **Koyama, Y., Wang, P., Liang, S., Iwaisako, K., Liu, X., Xu, J., Zhang, M. et al.**, Mesothelin/mucin 16 signaling in activated portal fibroblasts regulates cholestatic liver fibrosis. *J. Clin. Invest.* 2017. **127**: 1254–1270.

21 **Rinkevich, Y., Mori, T., Sahoo, D., Xu, P. X., Bermingham, J. R., Jr. and Weissman, I. L.**, Identification and prospective isolation of a mesothelial precursor lineage giving rise to smooth muscle cells and fibroblasts for mammalian internal organs, and their vasculature. *Nat. Cell. Biol.* 2012. **14**: 1251–1260.

22 **Zhang, N., Czepielewski, R. S., Jarjour, N. N., Erlich, E. C., Esaulova, E., Saunders, B. T., Grover, S. P. et al.**, Expression of factor V by resident macrophages boosts host defense in the peritoneal cavity. *J. Exp. Med.* 2019.

23 **Bot, J., Whitaker, D., Vivian, J., Lake, R., Yao, V. and McCauley, R.**, Culturing mouse peritoneal mesothelial cells. *Pathol. Res. Pract.* 2003. **199**: 341–344.

Abbreviations: **BMs**: bone marrow cells · **LPMs**: large peritoneal macrophages · **MCs**: mesothelial cells · **SPMs**: small peritoneal macrophages

Full correspondence: Dr. Stoyan Ivanov, Centre méditerranéen de médecine moléculaire - Université Côte d'Azur - INSERM U1065, Team 13, Nice, France
e-mail: stoyan.ivanov@unice.fr

Additional correspondence: Dr. Rodolphe Guinamard, Centre méditerranéen de médecine moléculaire - Université Côte d'Azur - INSERM U1065, Team 13, Nice, France
e-mail: rodolphe.guinamard@unice.fr

The peer review history for this article is available at https://publons.com/publon/10.1002/eji.201948164

Received: 22/2/2019
Revised: 7/5/2019
Accepted: 26/6/2019
Accepted article online: 28/6/2019

